


Optical superimposed vortex beams generated by integrated holographic plates with blazed grating

Cite as: Appl. Phys. Lett. **111**, 061901 (2017); <https://doi.org/10.1063/1.4997590>

Submitted: 08 April 2017 . Accepted: 23 July 2017 . Published Online: 08 August 2017

Xue-Dong Zhang, Ya-Hui Su, Jin-Cheng Ni, Zhong-Yu Wang, Yu-Long Wang, Chao-Wei Wang, Fei-Fei Ren, Zhen Zhang, Hua Fan, Wei-Jie Zhang, Guo-Qiang Li, Yan-Lei Hu, Jia-Wen Li , Dong Wu, and Jia-Ru Chu



View Online



Export Citation



CrossMark

ARTICLES YOU MAY BE INTERESTED IN

[Direct laser writing of complex microtubes using femtosecond vortex beams](#)

Applied Physics Letters **110**, 221103 (2017); <https://doi.org/10.1063/1.4984744>

[A highly efficient element for generating elliptic perfect optical vortices](#)

Applied Physics Letters **110**, 261102 (2017); <https://doi.org/10.1063/1.4990394>

[Three-level cobblestone-like TiO₂ micro/nanocones for dual-responsive water/oil reversible wetting without fluorination](#)

Applied Physics Letters **111**, 141607 (2017); <https://doi.org/10.1063/1.4998297>

Applied Physics Reviews
Now accepting original research

2017 Journal
Impact Factor:
12.894

AIP
Publishing

Optical superimposed vortex beams generated by integrated holographic plates with blazed grating

Xue-Dong Zhang,¹ Ya-Hui Su,¹ Jin-Cheng Ni,² Zhong-Yu Wang,² Yu-Long Wang,² Chao-Wei Wang,² Fei-Fei Ren,¹ Zhen Zhang,² Hua Fan,³ Wei-Jie Zhang,² Guo-Qiang Li,^{2,4} Yan-Lei Hu,² Jia-Wen Li,^{2,a)} Dong Wu,^{2,a)} and Jia-Ru Chu²

¹School of Electrical Engineering and Automation, Anhui University, Hefei 230601, China

²CAS Key Laboratory of Mechanical Behavior and Design of Materials, Department of Precision Machinery and Precision Instrumentation, University of Science and Technology of China, Hefei 230026, China

³Department of Mechanical and Electronic Engineering, Hefei University of Technology, Hefei 230009, China

⁴Key Laboratory of Testing Technology for Manufacturing Process of Ministry of Education, Southwest University of Science and Technology, Mianyang 621010, China

(Received 8 April 2017; accepted 23 July 2017; published online 8 August 2017)

In this paper, we demonstrate that the superposition of two vortex beams with controlled topological charges can be realized by integrating two holographic plates with blazed grating. First, the holographic plate with blazed grating was designed and fabricated by laser direct writing for generating well-separated vortex beam. Then, the relationship between the periods of blazed grating and the discrete angles of vortex beams was systemically investigated. Finally, through setting the discrete angle and different revolving direction of the holographic plates, the composite fork-shaped field was realized by the superposition of two vortex beams in a particular position. The topological charges of composite fork-shaped field ($l = 1, 0, 3, \text{ and } 4$) depend on the topological charges of compositional vortex beams, which are well agreed with the theoretical simulation. The method opens up a wide range of opportunities and possibilities for applying in optical communication, optical manipulations, and photonic integrated circuits. *Published by AIP Publishing.* [<http://dx.doi.org/10.1063/1.4997590>]

Optical vortices with helical phase wave-fronts carrying orbital angular momentum (OAM) have a phase winding factor described by $\exp(il\varphi)$, where φ is the azimuthal angle, l is the topological charge of optical vortex corresponding to an orbital angular momentum of $l\hbar$ per photon, and the positive or negative of topological charges represents different revolving direction of the phase fronts around the beam axis.¹ Optical vortex has shown great potential in modern optics and photonics due to their unprecedented promising applications in optical communication,² and optical manipulation.³ Researchers obtained vortex beam based on a few optical components such as spiral phase plates,⁴ q-plates,⁵ whispering gallery modes resonator,^{6–8} spatial light modulators (SLM),⁹ metasurfaces,^{10–12} and nano-fabricated holograms.^{1,13} In addition, when a vortex beam is superimposed with another one, the phase distribution of the composite vortex is dependent on the compositional vortex beams, and the superposed OAM states would also change due to the superposition of different vortex beams.¹⁴ The superposed OAM beams are possible to provide arbitrary OAM states for optical applications by increasing the number of composition OAM modes in the superposition. Recently, Wang *et al.* adopted a variable amplitude splitter and an OAM emitter were adopted generate the superposition of optical vortex beams.⁷ Moreover, a computer-generated hologram was utilized to produce the high-order superposed OAM modes for spinning object detection.⁹ But these methods significantly increase the complexity and volume of experimental systems. Therefore, a simple, efficient, and compact approach to achieve the superposition of two vortex beams is highly desirable.

In our work, we propose a compact strategy—two holographic plates with blazed grating (HPBGs) to realize the superposition of two vortex beams with controlled topological charges. Single HPBG ($\sim 60 \mu\text{m}$ size) was fabricated by direct laser writing, which can simultaneously generate and separate the first order optical vortices. Two HPBGs were used to generate superposed vortex beams by setting the discrete angle and revolving direction of every HPBG. Moreover, the relation between the topological charges of superposed vortex beams and compositional vortex beams was studied. The integrated HPBGs can be applied in optical tweezers,¹⁵ optical communication,¹⁶ and photonic integrated circuits.^{12,17,18}

A forked diffraction grating (the topological charges $l = 1$) was created by the phase distribution of the desired optical component plus a linear phase ramp,¹⁹ the whole structure consists of blazed grating and substrate [Figs. 1(a) and 1(b)]. The blazed grating was designed by using periodic gray value based on diffraction grating, which illustrates the blazed grating has grooves with a sawtooth-shaped profile. The thickness of sawtooth is defined as $h = \frac{\lambda}{n-n_0}$ with λ the wavelength of incident light, n (~ 1.504) the refractive index of HPBG, and n_0 (~ 1) the refractive index of air. d represents the grating period. The HPBG was fabricated by femtosecond-laser direct writing on photoresist (SZ2080, provided by FORTH, Greece).²⁰ Typical scanning electron microscopy (SEM) image of polymerized HPBG with a $60 \mu\text{m}$ diameter is shown in Fig. 1(c), which illustrates the fabricated structure is consistent well with the designed model. The measured thickness of sawtooth is $1.02 \mu\text{m}$ [The inset of Fig. 1(c)], which is in good agreement with theoretical value of $1.05 \mu\text{m}$. The sample was characterized by using a simple optical system [Fig. 1(d)]. The light

^{a)}Electronic addresses: jwl@ustc.edu.cn and dongwu@ustc.edu.cn

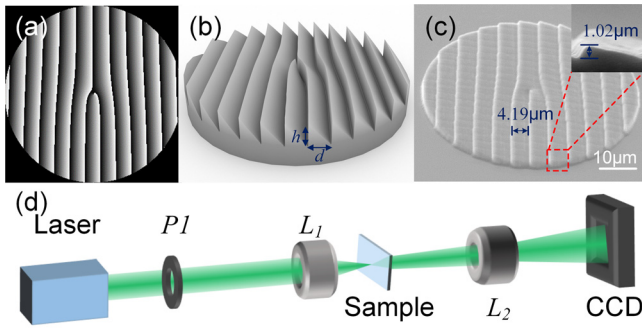


FIG. 1. (a) A forked diffraction grating with topological charge $l=1$ created by the phase distribution of the desired optical component plus a linear phase ramp. (b) The ideal three dimensional HPBG with a sawtooth-shaped profile consisting of blazed grating and substrate. The blazed grating was designed by using periodic gray value based on diffraction grating. (c) SEM images of a $60\ \mu\text{m}$ diameter. Inset: thickness profile extracted from the part of structure. $h=1.02\ \mu\text{m}$, $d=4.19\ \mu\text{m}$. (d) Schematic illustration of the optical performances detection setup.

from the $532\ \text{nm}$ wavelength laser was passed through a pinhole (PI) and objective lens L_1 (numerical aperture $NA=0.6$), and then focused on the sample (about 72% transmission efficiency). The generated vortex beam was collimated by objective lens L_2 ($NA=0.4$), and incident on a charge coupled device (CCD) camera.

A simple single beam original interferometric technique was adopted to characterize the phase singularity of the generated vortex beams, and the size of pinhole was adjusted to realize the interference of the vortex beam.⁴ Considering that the focal plane of the incident focused Gaussian beam is located at the Fresnel diffraction region, we can observe the transmitted diffraction patterns from HPBGs. The vortex beam diffracted into the m -th order acquires a singular phase with topological charge $q=m\cdot l$, and here, we will concentrate on the case of $m=1$. Schematic of HPBG with shifted vortex beam is shown in Fig. 2(a), from which we can observe the

generated vortex beam shift outside the laser spot without the reference beam. As shown in Figs. 2(b)–2(e), with the topological charge increasing, the central dark region becomes bigger and the donut ring becomes thinner. Then, we adjust the pinhole a little bigger so that the generated vortex beam interferes with the surrounding laser spot [Fig. 2(f)]. In Figs. 2(g)–2(k), we can find the central fringe of the interference pattern is obviously divided into l forks. The intensity of Gaussian beam peaks at the center, and it gradually weakens from center to edge, but the fringe contrast of interference is smallest at the center.²¹ Therefore, we can see that the central interference patterns are blurring, which are in good agreement with simulations [Figs. 2(g′)–(k′)].

To obtain a greater shifted distance from the center of HPBG, we studied the relationship between the periods of blazed grating and the discrete angles of vortex beams. The blazed grating usually concentrates as much of the incident light as possibly into only the first order by designing sawtooth-shaped profile. The shifted vortex beam depends on the sawtooth-shaped profile, which has two important parameters: the thickness and the grating period. According to the gray value change of designed hologram and a $60\ \mu\text{m}$ diameter HPBG, we theoretically calculate the grating period d_i , which can be expressed as

$$d_i = \frac{51}{i\pi}, \quad (1)$$

where $i=2, 3, 4$, and 5 (the generated vortex beam need to shift outside the laser spot, $i>1$). According to Eq. (1), we can obtain $d_2=8.12\ \mu\text{m}$, $d_3=5.41\ \mu\text{m}$, $d_4=4.06\ \mu\text{m}$, $d_5=3.25\ \mu\text{m}$, and the theoretical values are consistent with the experimental results [Fig. 1(c)]. The diffracted beams propagate at the discrete angles, which can be expressed as

$$\theta_i = \frac{\lambda}{d_i}, \quad (2)$$

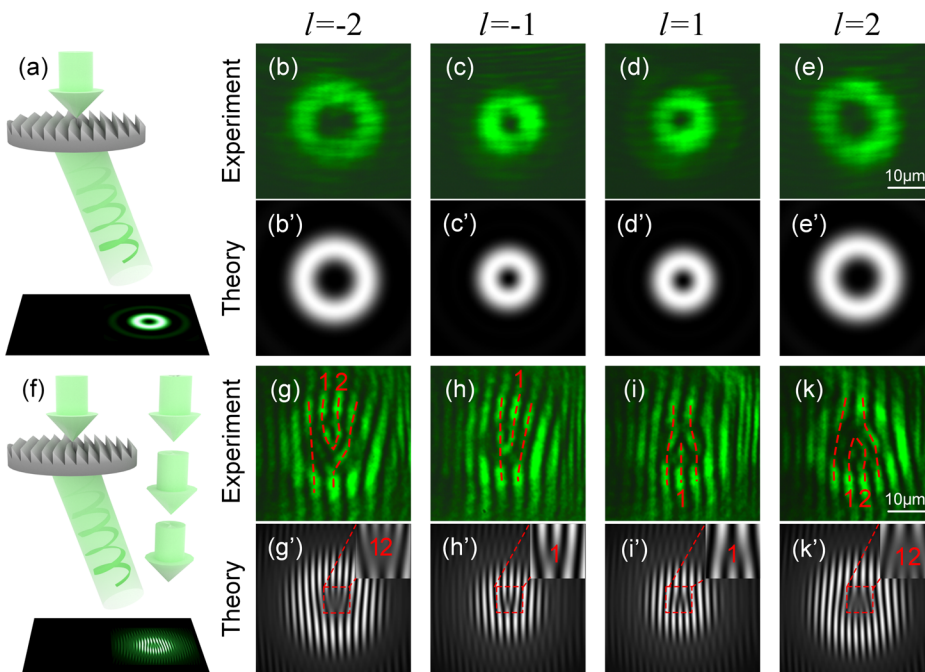


FIG. 2. (a) Schematic illustration of HPBG with shifted vortex beam, the generated vortex beam shift outside the laser spot without the reference beam. (b)–(e) Experimental and theoretical far field intensity patterns of the generated vortex beam with topological charge $l=-2, -1, 1$, and 2 . (f) The generated vortex beam interferes with the surrounding laser spot. (g)–(k) Experimental and theoretical interference patterns of the generated vortex beam and the reference beam, the central fringe of the interference pattern is obviously divided into l forks. The theoretical patterns match well with the observed ones.

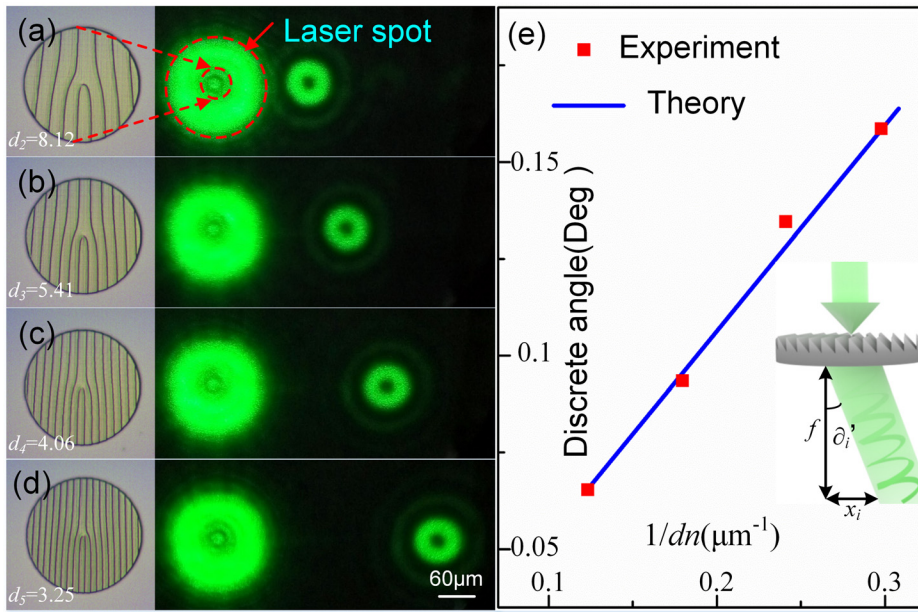


FIG. 3. (a)–(d) Microscope patterns of HPBG with different grating periods. The smaller the grating periods, the greater the shifting distances of the generated vortex beams. The shaded part of the red circle is the location of the structure, and the large red circle is the location of a laser spot. (e) The theoretical ∂_i (the blue line) compares to experimental ∂'_i (the red dot). The inset shows that the generated vortex beam shift the center of HPBG.

where λ is the wavelength of incident light. So, the different grating periods can produce different discrete angles, and the vortex beams with different discrete angles correspond to different shifted distances. For applications requiring isolated vortex beams, it is necessary to use holograms with small grating periods. Different transmission HPBGs with grating periods of d_2 , d_3 , d_4 , and d_5 (the topological charge $l=2$ and $60\ \mu\text{m}$ diameter) were fabricated, as shown in Figs. 3(a)–3(d). The HPBG with different grating periods can produce different shifting distances, and the smaller the grating periods, the greater the shifting distances. The shaded part of the red circle is the location of the structure, and the generated vortex beam can be shifted out of the laser spot. According to the shifting distance, we can experimentally calculate the discrete angles, which can be expressed as

$$\partial'_i = \frac{x_i}{f}, \quad (3)$$

where x_i is the shifted distances corresponding to different grating periods, and f is the distance between the sample and the observation screen [the inset of Fig. 3(e)]. After measuring x_i and f , discrete angles were obtained, which show a good agreement with theoretical calculations [Fig. 3(e)].

The m -th diffraction order can be divided into positive and negative diffraction orders. These negative diffraction orders propagating to one side of the central order beam have quantized OAM that is antiparallel to the propagation direction, and vice versa for positive diffraction orders.¹ We defined that positive diffraction orders propagate to the right side of the central order beam, so the superposition of two vortex beams is the superposition of the positive diffraction order of vortex beam and the negative diffraction order of another vortex beam (here we will concentrate on the case $m = +1, -1$). The superposed light field can be considered a kind of composite fork-shaped field. The topological charges of composite fork-shaped field are equal to the sum of two topological charges, which can be expressed as

$$l = (+l_1) + (-l_2), \quad (4)$$

where “+” and “−” represent the positive and negative diffraction orders of vortex beams, respectively. Further, when two vortex beams with different phase distribution are appropriately weighted to give the different intensity distributions, the relative phases of these two modes can be interactional in composite field so that they interfere destructively at their common focus to give forked intensity distribution. Two vortex beams with topological charges $l_1=2$ and $l_2=2$ can be superposed. Figure 4(a) shows a SEM image of $4.06\ \mu\text{m}$ -period HPBGs with different revolving directions, in which the left one is the counterclockwise rotation of 60° and the right one is counterclockwise rotation of 120° . A schematic illustration of superposition of two vortex beams is shown in Fig. 4(b). Through setting the discrete angle and different revolving direction of the holographic plates, those two vortex beams can be superposed in a fixed space diffraction distance, and the CCD is placed at the designed diffraction distance and detect the superposition of two OAM beams. The topological charge of composite fork-shaped field [$l=0$, Fig. 4(e)] is created by the superposition of the positive diffraction order of vortex beam with topological charge $l_1=2$ and the negative diffraction order of vortex beam with topological charge $l_2=2$. The superposed patterns of other different topological charges [$l(l_1=1, l_2=2)=-1$, $l(l_1=1, l_2=-2)=3$, and $l(l_1=2, l_2=-2)=4$] are shown in Figs. 4(c), 4(d), and 4(f), which are well agreed with the theoretical result of composite fork-shaped field [Figs. 4(g)–4(j)]. The phase distributions of composite fork-shaped field are shown in Figs. 4(k)–4(n). The composite OAM states are determined by component vortex beams with different topological charges, while the topological charges can only be changed by switching HPBG with different topological charges. In order to obtain larger OAM, we can simply integrate two HPBGs with two smaller the topological charges. Here, our proposed approach is very robust, since it not only overcomes complex experimental setup problems of conventional ways for producing OAM superposition, such as Segnac interferometer²² consisting of an OAM beam generator, beam splitters, Dove prism, and mirrors, but also efficiently

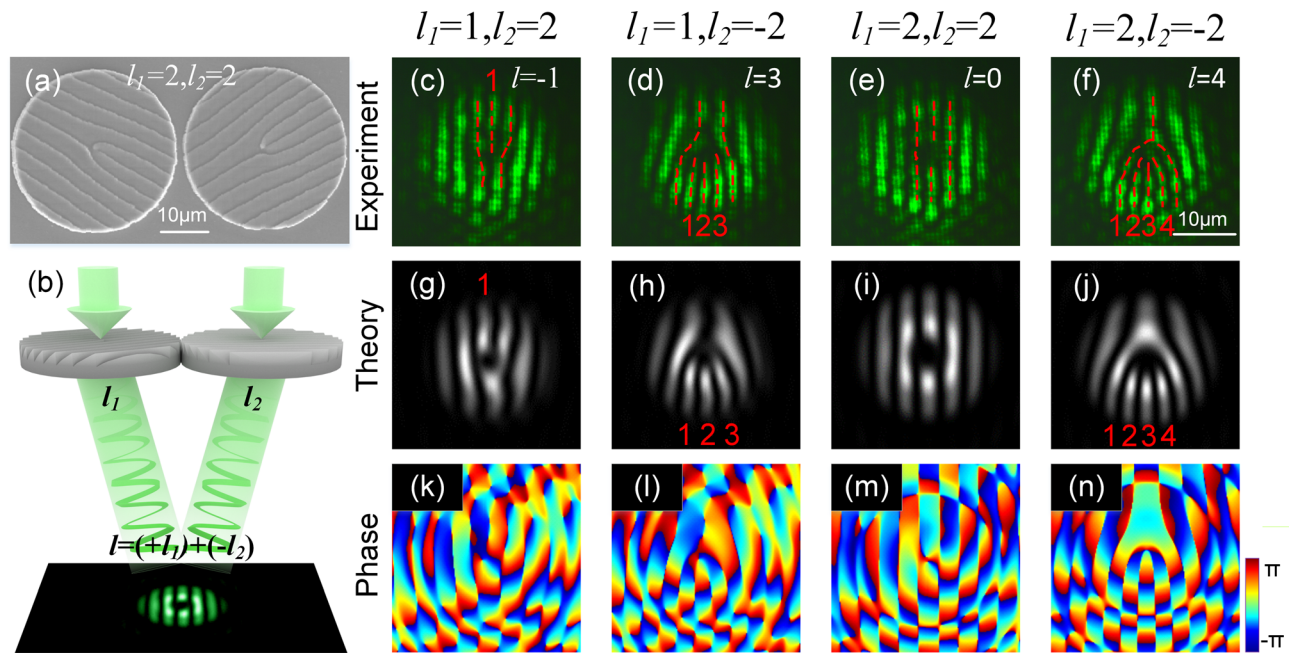


FIG. 4. (a) A SEM image of integrated HPGs with different revolving direction, and the diameter and grating periods of single structure are $40 \mu\text{m}$ and $4.06 \mu\text{m}$. (b) Schematic illustration of superposition of two vortex beams. (c)–(f) The superposed patterns of the generated vortex beams with different topological charges. The topological charges of composite fork-shaped field ($l = -1, 0, 3$, and 4) is equal to the sum of two topological charges. (g)–(j) Theoretical results correspond to (c)–(f). (k)–(n) The phase distributions of the composite fork-shaped field. The theoretical patterns match well with the observed ones.

generates composite OAM beams with controlled topological charges.

In conclusion, we experimentally and theoretically demonstrate that the superposition of two vortex beams can be achieved by integrating HPGs with different revolving direction and setting the discrete angle. The smaller-size ($\sim 60 \mu\text{m}$) HPG with controlled topological charges fabricated by high fidelity direct laser polymerization can be used simultaneously to generate and separate vortex beam. The relationship between the blazed grating with different grating periods and its discrete angles was also investigated. In addition, we have demonstrated that the superposition of two vortex beams is the superposition of the positive diffraction order of vortex beam and the negative diffraction order of another vortex beam, and the OAM states of composite fork-shaped field are determined by the topological charges of compositional vortex beams. Due to the simplicity of our design, this method not only overcomes complex experimental setup problems of conventional ways, but also efficiently generates composite OAM beams with controlled topological charges.

This work was supported by National Natural Science Foundation of China (Grant Nos. 51275502, 61475149, 51405464, 91223203, 61377006, 91423103, and 11204250), Anhui Provincial Natural Science Foundation (Grant No. 1408085ME104), National Basic Research Program of China (Grant No. 2011CB302100), the Fundamental Research Funds for the Central Universities (WK2480000002), and “Chinese Thousand Young Talents Program.”

¹B. J. McMorran, A. Agrawal, I. M. Anderson, A. A. Herzing, H. J. Lezec, J. J. McClelland, and J. Unguris, *Science* **331**, 192 (2011).

²J. Wang, J.-Y. Yang, I. M. Fazal, N. Ahmed, Y. Yan, H. Huang, Y. X. Ren, Y. Yue, S. Dolinar, M. Tur, and A. E. Willner, *Nat. Photonics* **6**, 488 (2012).

³M. Padgett and R. Bowman, *Nat. Photonics* **5**, 343 (2011).

⁴E. Brasselet, M. Malinauskas, A. Žukauskas, and S. Juodkakis, *Appl. Phys. Lett.* **97**, 211108 (2010).

⁵Y. G. Zhao, Z. P. Wang, H. H. Yu, S. D. Zhuang, H. J. Zhang, X. D. Xu, J. Xu, X. G. Xu, and J. Y. Wang, *Appl. Phys. Lett.* **101**, 031113 (2012).

⁶Q. S. Xiao, C. Klitis, S. Li, Y. Chen, X. Cai, M. Sorel, and S. Y. Yu, *Opt. Express* **24**, 3168 (2016).

⁷Y. Wang, X. Feng, D. Zhang, P. Zhao, X. Li, K. Cui, F. Liu, and Y. D. Huang, *Sci. Rep.* **5**, 10958 (2015).

⁸X. L. Cai, J. W. Wang, M. J. Strain, B. Johnson-Morris, J. B. Zhu, M. Sorel, J. L. O’Brien, M. G. Thompson, and S. Y. Yu, *Science* **338**, 363 (2012).

⁹M. P. J. Lavery, F. C. Speirits, S. M. Barnett, and M. J. Padgett, *Science* **341**, 537 (2013).

¹⁰J. B. Sun, X. Wang, T. Xu, Z. A. Kudyshev, A. N. Cartwright, and N. M. Litchinitser, *Nano Lett.* **14**, 2726 (2014).

¹¹M. Q. Mehmood, S. Mei, S. Hussain, K. Huang, S. Y. Siew, L. Zhang, T. H. Zhang, X. H. Ling, H. Liu, J. H. Teng, A. Danner, S. Zhang, and C.-W. Qiu, *Adv. Mater.* **28**, 2533 (2016).

¹²J. W. Zeng, L. Li, X. D. Yang, and J. Gao, *Nano Lett.* **16**, 3101 (2016).

¹³V. Grillo, G. C. Gazzadi, E. Karimi, E. Mafakheri, R. W. Boyd, and S. Frabboni, *Appl. Phys. Lett.* **104**, 043109 (2014).

¹⁴I. D. Maleev and G. A. Swartzlander, *J. Opt. Soc. Am. B* **20**, 1169 (2003).

¹⁵C. H. J. Schmitz, K. Uhrig, J. P. Spatz, and J. E. Curtis, *Opt. Express* **14**, 6604 (2006).

¹⁶G. Gibson, J. Courtial, M. J. Padgett, M. Vasnetsov, S. M. Barnett, and S. Franke-Arnold, *Opt. Express* **12**, 5448 (2004).

¹⁷N. M. Litchinitser, *Science* **337**, 1054 (2012).

¹⁸M. J. Strain, X. L. Cai, J. W. Wang, J. B. Zhu, D. B. Phillips, L. F. Chen, M. Lopez-Garcia, J. L. O’Brien, M. G. Thompson, M. Sorel, and S. Y. Yu, *Nat. Commun.* **5**, 4856 (2014).

¹⁹A. M. Yao and M. J. Padgett, *Adv. Opt. Photonics* **3**, 161 (2011).

²⁰D. Wu, J.-N. Wang, L.-G. Niu, X. L. Zhang, S. Z. Wu, Q.-D. Chen, L. P. Lee, and H. B. Sun, *Adv. Opt. Mater.* **2**, 751 (2014).

²¹S. Li and Z. Wang, *Appl. Phys. Lett.* **103**, 141110 (2013).

²²A. Vaziri, G. Weihs, and A. Zeilinger, *J. Opt. B: Quantum Semiclassical Opt.* **4**, S47 (2002).